

Deep Neural Network for Magnetic Core Loss Estimation using the MagNet Experimental Database

Xiaobing Shen, Hans Wouters, Wilmar Martinez

KU Leuven – EnergyVille

Department of Electrical Engineering (ESAT)

Leuven - Genk, Belgium

Email: xiaobing.shen, hans.wouters, wilmar.martinez@kuleuven.be

Keywords

«Magnetic Device», «Machine Learning», «Core Loss Modelling», «Neural Network».

Abstract

Magnetic components play a critical role in power electronics systems and their evolution towards higher power density and efficiency. Nevertheless, accurately modelling magnetic core losses is not a trivial task, requiring extensive measurements. In the context of the general advances of Machine Learning technologies in power electronics applications, this paper presents a Deep Neural Network (DNN) approach to core loss estimations. Various internal parameters of the DNN are tested and compared, to identify the optimal DNN structure for the core loss estimation, including the number of hidden layers, number of neurons, data transformation, and different activation functions. The training data-set comprises the MagNet database for N87 toroid magnetic cores, based on an experimental data acquisition system capable of automatically measuring various magnetic cores under arbitrary excitation signals. The results of the DNN models indicate that a DNN with suitable parameters can robustly and accurately model the core losses. The attainable accuracy is well within the required range for magnetic core losses. The optimal structure proposed in this paper consists of 10 hidden layers with sigmoid activation functions, 10 neurons in each layer, integrating a log-transformation and data normalization. The model is validated with extensive experimental tests similar to the MagNet measurement system. Furthermore, tests at higher switching frequencies up to 1MHz indicate that the model can predict losses for parameters outside the range of its training data. With the achieved performance, the DNN can benefit various power electronics engineering challenges such as loss estimation for inductor design.

Introduction

Core loss estimation is not a trivial task and due to its complexity, it is not an entirely solved matter neither. Although magnetic characterization has been studied extensively for over a century, the distinctive conditions in power electronics have introduced many new challenges. This imposes an important area of research, as magnetic components play a critical role in most power electronic applications. These new challenges for the characterization, modelling and measurements of magnetic components arise from various developments. Where traditionally, the excitation of such magnetic materials has dominantly been sinusoidal, various modulation control methods such as pulse width modulation (PWM) in power electronics lead to a diversity of excitation waveforms [1]. Because of this modulation, they generally contain a significant amount of harmonic content [2]. Furthermore, advances in semiconductor technology towards wide bandgap devices have led to an increase in switching frequencies into the MHz range in order to realize compact power converters [3].

Different models and equations have historically been used to characterize magnetic materials. Many of these parameters can be traced back to the relationship between the magnetic flux density in the material

and the applied magnetic field strength. The magnetic permeability of the material relates these quantities in the BH curve, often referred to as the hysteresis loop. An established model to characterize the hysteresis loop is the Steinmetz equation, first introduced in 1892 [4]. Many variations of this equation are developed, to broaden the range in which the equation applies and to take various additional parameters into account such as temperature, frequency, and the type of excitation [5], [6]. One of the most recent advances is the Steinmetz Premagnetization Graph presented in [7], based on the improved Generalized Steinmetz Equation (iGSE) [8]. This considers non-sinusoidal excitation, as well as the effect of DC magnetic flux bias. These models, however, are computationally expensive, require specific material properties, and often require extensive measurements.

Recently, novel methodologies based on Machine Learning (ML) are researched for characterizing the core losses [1], [9]-[11], as these algorithms are proven to be effective in solving nonlinear problems [12]. The concept of Deep Neural Networks (DNN), first proposed by G.E. Hinton et al. [13], refers to a machine learning process that obtains a multi-level deep network structure, based on sample data [14]. DNNs, as a new research field of ML, gains breakthroughs in applications such as speech recognition and computer vision. This paper presents a Deep Neural Network based approach and investigates the effect of the many parameters that can be fine-tuned in the DNN, to provide a robust and accurate model.

Data-set for DNN Model

Machine learning algorithms are to a large extent data based. With larger data-set, better performances in the training process of a DNN will be achieved. This paper presents a DNN based on the MagNet database [12]. Analogous to the ImageNet database [15], which is widely used in computer vision and general deep learning research, MagNet provides data for various magnetic research purposes. It is based on a data acquisition system capable of automatically generating large data-sets. The measurement setup is shown in Fig. 1. The power stage of this setup can generate arbitrary excitation waveforms. The main components consist of a power amplifier (V_1) to generate sinusoidal excitations, a single-phase bridge (Q_s) to generate the PWM excitations, and AO4444 MOSFETs for all power switches. Various magnetic components can be connected as devices under testing (DUT), including varying geometries, materials, and sizes. Measurements are made of the current through the primary winding and voltage over the secondary winding. Shunt resistors are used for the current measurements, voltage dividers for the voltage measurements.

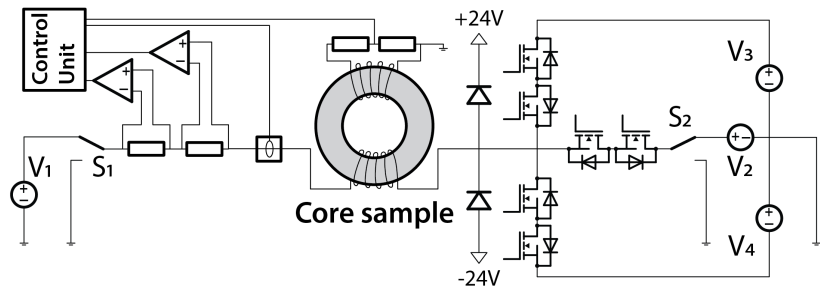


Fig. 1: MagNet magnetic core loss measurement setup

In this paper, the MagNet database is limited to data on toroid cores N87 material. A hypothesis of [12] is that the physics that govern the core loss for a material, are analogous for similar materials. Therefore, knowledge gained of magnetic characterization using a certain waveform or material, can be used as input for characterizing similar materials and/or with different waveforms. This hypothesis will be tested against the constructed DNN. This paper uses the data-set acquired by applying a sinusoidal excitation on the N87 toroid as DUT, as this is popularly used in power electronics. The frequency range of the data-set is 10kHz to 500kHz. The duty ratio is fixed, at a constant 0.50 value. The data-set provides the flux density [mT] and power loss density [kW/m³] as a function of the frequency [Hz], totaling over 10,000 data-points.

DNN Model Structure and Optimization

As illustrated in Fig. 2a, the starting point of the algorithm is a function with unknown parameters. The equations governing the magnetic losses, however, are complicated and contain many parameters characterizing the material properties, geometry, excitation waveform, etc. This large number of unknown parameters is defined as , alongside a loss function $L(\theta)$ for each of them. This loss indicates the approximation of the estimate values from their true value. Then, the gradient decent method is used, a linear iterative optimization algorithm which is established in both linear and nonlinear problems due to its robust convergence properties. With it, the minima of the loss function are located, providing the optimal solutions for minimum losses and their parameters θ . These are the unknown parameters required for the model to accurately compute the core losses for new inputs.

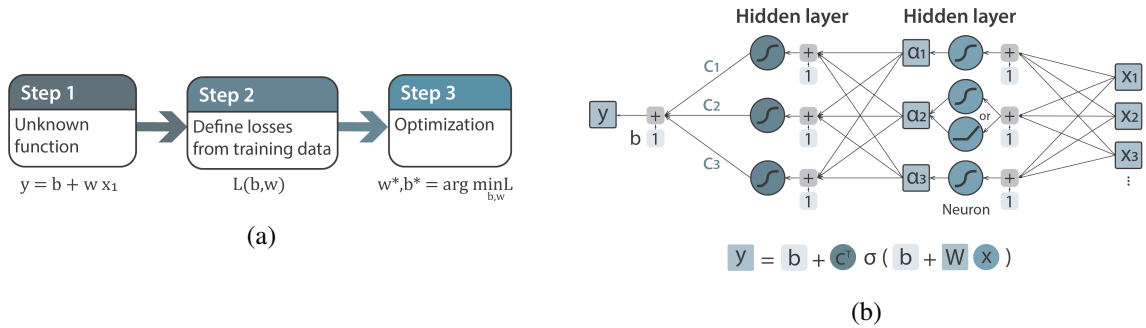


Fig. 2: (a) General training workflow in machine learning, (b) General DNN structure

A DNN structure is proposed based on the workflow of machine learning. Fig. 2b shows the typical structure of a DNN, containing multiple inputs and outputs. Different neurons and layers are connected, resulting in a neural network. The last layer has a fixed number of neurons, representing the number of outputs. The rest of the layers are the hyperparameters of the structure, also named hidden layers. With the expansion of the number of neurons and layers, the DNN strengthens its processing power for more complex data. The required computation time, however, also increases along with its complexity, resulting in a trade-off.

Other important hyperparameters are the batch and epoch number. The batch size stands for the number of samples processed per training iteration. Each sample is one measurement of the magnetic losses and flux density as a function of the excitation frequency. An epoch is comprised of multiple batches and represents the number of times the DNN iterates over all samples.

Furthermore, the DNN training process involves splitting the data-set of the magnetic core losses into the training and validation set. In this paper, 10-fold cross validation is employed, which implies a random partition and classification of the original core loss data-set. After initializing the weights and biases of the DNN and the hyperparameters, the mean square error (MSE) is used to evaluate the accuracy of the DNN and update its parameters in an iterative manner.

DNN Analysis Parameters

The DNN structure is physical-free as discussed above. To prevail over alternative data processing and optimization algorithms, a robust, flexible, and accurate DNN is required, especially for power electronics. Structural parameters of the DNN can significantly influence its behavior, including: (1) the structure of DNN, i.e., choices of activation function, neurons, and hidden layers; (2) data scaling techniques such as input and output data normalization and transformation; (3) training processing, including the splitting method and optimization algorithm on the data. This paper evaluates five different DNN structures, as described in Table I.

Table I: Overview of the DNN analysis parameters

Model ID	Hidden layers	Neurons	Data transformation	Data normalisation	Activation function
M1	1	1	None	None	None
M2	2	5+1	None	None	Sigmoid
M3	2	5+1	Log	Yes	Sigmoid
M4	5	5+1	Log	Yes	Sigmoid
M5	10	5+1	Log	Yes	Sigmoid

Results of Selected DNN Structures

According to the wide range of parameters presented in Table II, the proposed DNN models are investigated in MATLAB, making intensive use of its NN-toolbox. All DNNs detailed above are validated by a 10-fold cross-validation. The results are displayed in Fig. 3 and summarized in Table II, providing the difference in the resulting errors and the epoch number at which the best validation performance (BVP) is reached.

Table II: Overview of the DNN analysis parameters

Model ID	Max. error	RMS error	BVP epoch no.
M1	/	/	7
M2	25.10%	13.70%	914
M3	0.53%	0.04%	108
M4	0.28%	0.00%	21
M5	0.18%	0.00%	42

Model 1, with no data transformation or normalization, nor any layers and neurons, is a simple and well-known linear regression model. it provides fast convergence but low performance, as shown in Fig. 3a. The MSE of M2 is shown in Fig. 3b. Compared to model 1, it consists of 2 hidden layers with sigmoid activation functions, 5 neurons for the hidden layer, and 1 neuron for the output layer. As visible in the graph, this drastically decreases the MSE. The epoch number, however, increases significantly as well.

Considering that the 2-dimensions of inputs have a wide range of magnitude, which may result in numerical problems for a model, data normalization and log-transformation for both input data and output data are implored. This scales the data-set, improving the accuracy of the training process while also increasing the training speed. Hereby, model 3 with the same number of neurons and layers as model 2 performs significantly better. This is illustrated in Fig. 3c.

Furthermore, the MSE of models 4 and 5 are shown in Fig. 3d and Fig. 3e respectively. Compared with the third model, M4 and M5 go deeper with 5 and 10 hidden layers. The results show that M5 with data normalization, log-transformation and 10 layers shows the best performance. Thus, one can conclude that by going deeper while using data transformation, higher performance can be obtained.

In summary, a deeper structure and variable processing methods (variable normalization and transformation) contribute to a more robust and accurate DNN. More specifically, with variable processing methods, the performance improves dramatically. However, there is a limit to how deep the model should go to obtain acceptable accuracy. In our specification, 5 layers with data processing techniques, as introduced above, are acceptable to build a fully connected DNN for magnetic core loss estimation, based on the MagNet database. Moreover, to get a deeper structure as opposed to a ‘fatter’ DNN, a ‘skinny’ DNN is maintained by fixing the number of neurons in each layer.

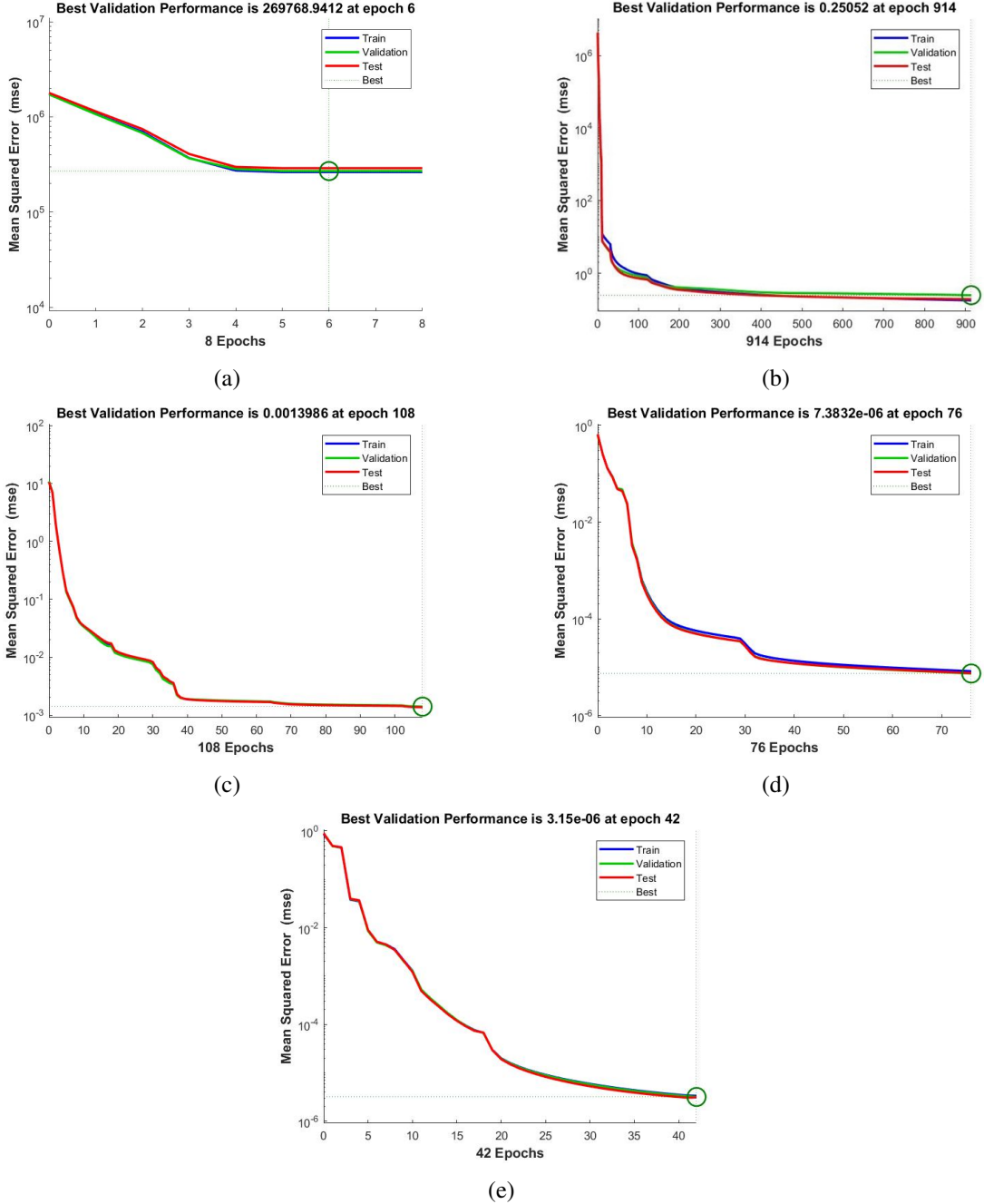


Fig. 3: MSE of the different DNNs, (a) model 1, (b) model 2, (c) model 3, (d) model 4, (e) model 5

Experimental Comparison

To validate both the MagNet measurement data and the DNN model, extensive experimental validation is conducted. The DUT in these experiments is a N87 toroid core. The R25 size is selected and 32 windings are used, as shown in Fig. 4c. A high frequency full-bridge GaN inverter produces the excitation signals with the same frequency and duty cycle as used in the MagNet database. This measurement setup is shown in Fig. 4a. Both the current through the DUT and the induced voltage over a secondary winding are measured, which excludes the effect of the DUT's resistance from the voltage measurement. The data is then processed to construct the BH-curve, and subsequently calculate the core losses. As such, both the training data and the DNN output can be validated. Furthermore, this is also used to test the ability of the DNN for accurately predicting core losses outside the range of its training data. Therefore, measurements are done at switching frequencies of 500kHz to 1MHz as well.

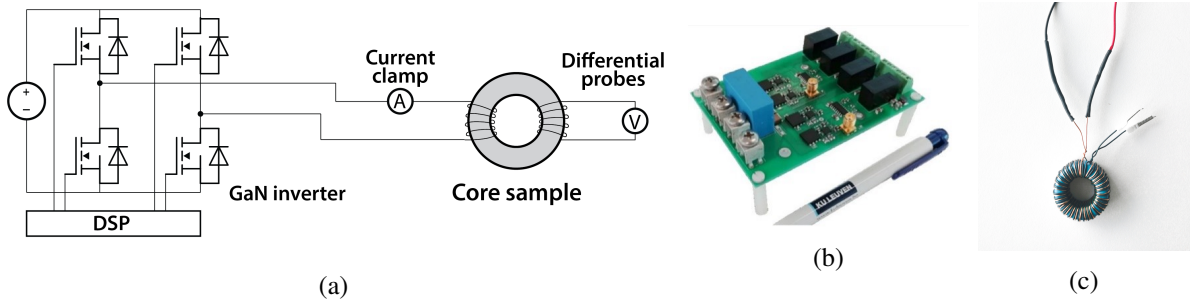


Fig. 4: (a) Measurement setup schematic, (b) GaN inverter and control circuit, (c) Toroid N87 R25 DUT

To perform the measurements, the GaN inverters are controlled by a 150MHz DSP with a unipolar modulation, shown in Fig. 4b. The inverter works within a frequency range of 10 kHz to 1MHz. The current through the primary winding and the voltage over the secondary are measured by an oscilloscope capable of collecting 10M points per measurement with a maximum sampling frequency of 2.5 GS/s real time. Fig. 3a shows the measured currents and voltages at a 50Hz fundamental frequency with varying carrier frequencies and a fixed magnetic flux density of 200mT in the DUT.

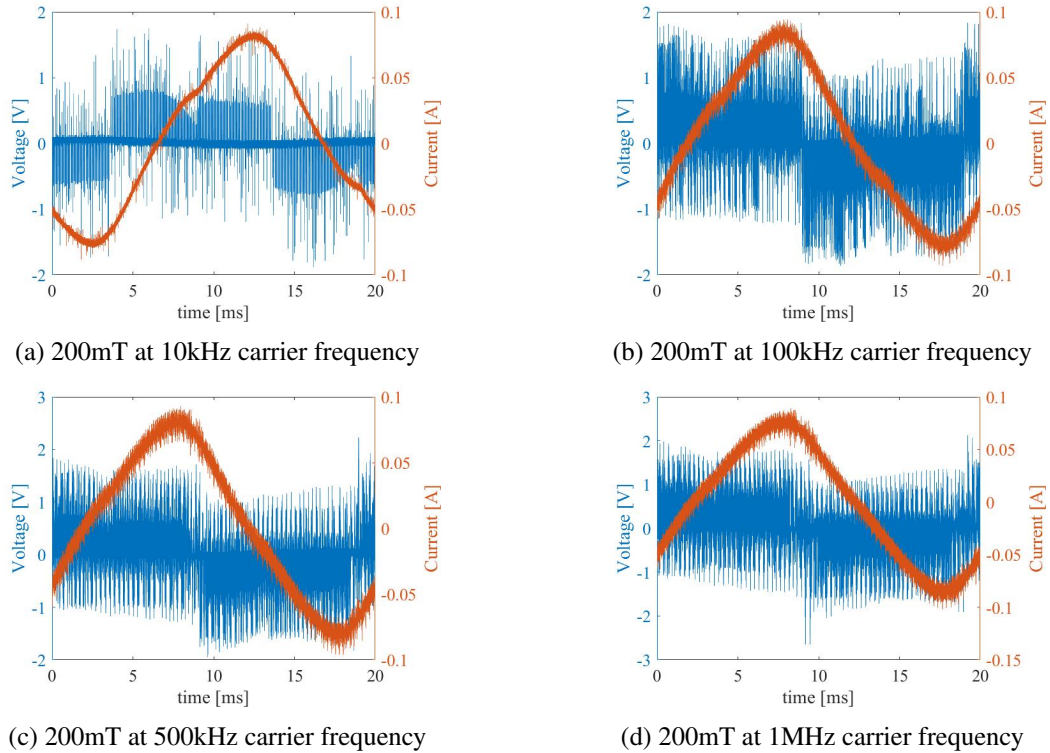


Fig. 5: Measured current and voltage waveforms of the DUT at 50 Hz fundamental frequency

Based upon the collected data, the flux density and core losses within the frequency range of 10kHz-1MHz are determined. Hereby, the BH-curves at different frequencies are derived as well, as shown in Fig. 6a. The flux density can be obtained from the induced voltage over the secondary winding using Faraday's law, provided in equation (1). In addition, the magnetic field strength in the inductor can be derived from the current through the primary winding based on Ampère's law, see equation (2).

$$B(t) = \frac{1}{N_2 A_e} \int v_2(t) dt \quad (1)$$

$$H(t) = \frac{N_1 i_1(t)}{l_e} \quad (2)$$

Here, N_1 and N_2 are the number of turns of the primary and secondary winding respectively, A_e is the effective area of the core, and l_e is the length of the main flux path. These can be combined to calculate the magnetic core loss density in equation (3), based on the detailed mathematical procedure in [16]:

$$P_{Fe} = \frac{N_1 f}{N_2 A_e l_e \rho} \int_0^1 i_1(t) v_2 dt \quad (3)$$

where ρ is the material mass density, which for N87 is equal to 4850 kg/m^3 . Due to the sinusoidal voltage, the induced magnetic flux density will be of sinusoidal shape as well. This leads to the BH-curves as shown in Fig. 6a and the magnetic losses of Fig. 6b as a function of the switching frequency.

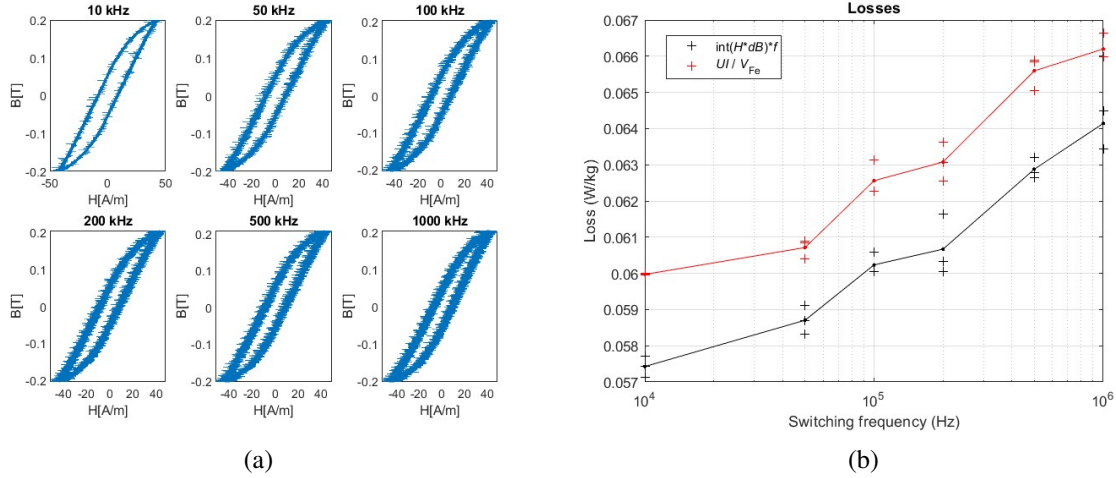


Fig. 6: Measurement (a) BH-curves and (b) Magnetic losses at $B_{max} = 200\text{mT}$ for the N87 R25 toroid

As such, at a certain switching frequency such as 1MHz, the magnetic losses can be predicted for an entire range of flux densities, as illustrated in Fig. 7. This shows a comparison between the measured results and the DNN model for different flux densities at a fixed switching frequency of 1MHz. As such, it provides the error distribution of the DNN model at different flux densities.

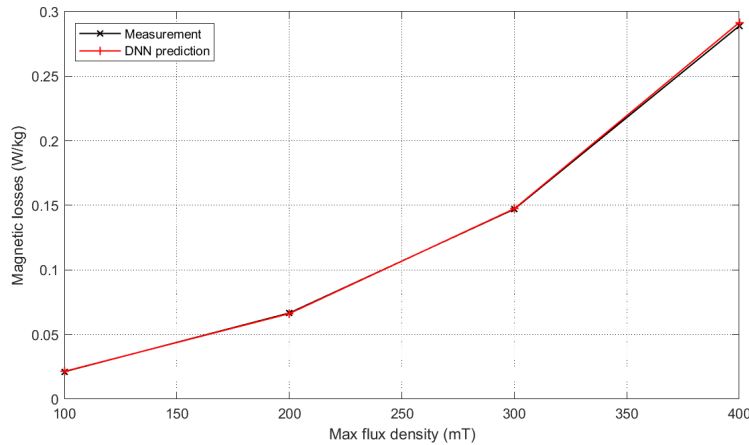


Fig. 7: Comparison of the measured and predicted losses for a switching frequency of 1MHz

It can be observed that the error is relatively small, with an error of only 0.2% at 1MHz and 300mT. The maximum error is 0.90%, at the maximal flux density of 400mT. This larger error at higher flux densities is an expected outcome, due to the nonlinear behavior of the core when saturating. Furthermore, these accurate results at 1MHz indicate the possibility of using the DNN model in high frequency applications such as magnetic design for high frequency power converters and LC filters. As such, the fast model can be used to analyze and reduce the losses in magnetic components. The trained DNN model could work as a surrogate model for the characterization of these magnetic losses.

Conclusion

This paper explores the potential of Deep Neural Networks to solve the complex challenges arising from the calculation of magnetic core losses. By comparing different DNN structures, a new DNN model based on experimental data is presented and validated. Developmental procedures of the DNN model are discussed, such as data processing, cross-validation, and deep layers with fixed neurons. The results indicate that the resulting DNN-based model is capable of producing accurate results compared to the experimental magnetic core measurements. The accuracy obtained is well within the acceptable range for magnetic core loss estimation. Its use in high frequency applications is experimentally validated at up to 1MHz, as well as the use of the DNN model for switching frequencies outside of the range of its training data.

Future work could be done on improving the DNN model to capture more scenarios, such as different excitation waveforms, a wider range of input frequencies, and different core materials, shapes and sizes. With more measurement data, the model can be further enhanced and optimized. As for magnetic design, it could function as a surrogate model, which yields the same behaviors and performance as existing magnetic loss models while reducing the number of required measurements and setups. This way, the computational and testing efforts can be reduced. The proposed structure is envisioned to be implemented for magnet loss estimation for inductor and transformer design and optimization, as it can provide a well-trained, robust, and accurate model.

References

- [1] Z. Zhao et al., "Modeling Magnetic Hysteresis Under DC-Biased Magnetization Using the Neural Network," *IEEE Trans. Magn.*, vol. 45, no. 10, pp. 3958–3961, Oct. 2009, doi: 10.1109/TMAG.2009.2023070
- [2] W. Martinez and C. Suarez, "Total Harmonic Distortion Analysis in Magnetic Characterization using High Frequency GaN Inverter in the MHz Order," in *EPE '19 ECCE Europe*, Sep. 2019, p. P.1-P.9. doi: 10.23919/EPE.2019.8915546
- [3] M. Parvez et al., "Wide Bandgap DC-DC Converter Topologies for Power Applications," *Proc. IEEE*, vol. 109, no. 7, pp. 1253–1275, Jul. 2021, doi: 10.1109/JPROC.2021.3072170
- [4] J Chas. P. Steinmetz, "On the Law of Hysteresis," *Trans. Am. Inst. Electr. Eng.*, vol. IX, no. 1, pp. 1–64, Jan. 1892, doi: 10.1109/T-AIEE.1892.5570437
- [5] J. Reinert, A. Brockmeyer, and R. De Doncker, "Calculation of losses in ferro- and ferrimagnetic materials based on the modified Steinmetz equation," *IEEE Trans. Ind. Appl.*, vol. 37, no. 4, pp. 1055–1061, Jul. 2001, doi: 10.1109/28.936396
- [6] J. Li, T. Abdallah, and C. R. Sullivan, "Improved calculation of core loss with nonsinusoidal waveforms," in *IEEE 36th IAS Annual Meeting*, Sep. 2001, vol. 4, pp. 2203–2210 vol.4. doi: 10.1109/IAS.2001.955931
- [7] J. Mu "hlethaler et al., "Core losses under DC bias condition based on Steinmetz parameters," in *The 2010 ECCE ASIA -*, Jun. 2010, pp. 2430–2437. doi: 10.1109/IPEC.2010.5542385
- [8] K. Venkatachalam et al., "Accurate prediction of ferrite core loss with nonsinusoidal waveforms using only Steinmetz parameters," *CIPE*, 2002. Proceedings., Jun. 2002, pp. 36–41. doi: 10.1109/CIPE.2002.1196712
- [9] J. I. Kucuk, "Prediction of hysteresis loop in magnetic cores using neural network and genetic algorithm," *J. Magn. Magn. Mater.*, vol. 305, no. 2, pp. 423–427, Oct. 2006, doi: 10.1016/j.jmmm.2006.01.137
- [10] X. Zhao and Y. Tan, "Modeling Hysteresis and Its Inverse Model Using Neural Networks Based on Expanded Input Space Method," *TCST.*, vol. 16, no. 3, pp. 484–490, 2008, doi: 10.1109/TCST.2007.906274
- [11] S. Shimokawa et al., "Fast 3-D Optimization of Magnetic Cores for Loss and Volume Reduction," *IEEE Trans. Magn.*, vol. 54, no. 11, pp. 1–4, Nov. 2018, doi: 10.1109/TMAG.2018.2841364
- [12] H. Li et al., "MagNet: A Machine Learning Framework for Magnetic Core Loss Modeling," in *2020 IEEE 21st COMPEL*, Nov. 2020, pp. 1–8. doi: 10.1109/COMPEL49091.2020.9265869
- [13] G. E. Hinton, S. Osindero, and Y.-W. Teh, "A fast learning algorithm for deep belief nets," *Neural Comput.*, vol. 18, no. 7, pp. 1527–1554, Jul. 2006, doi: 10.1162/neco.2006.18.7.1527
- [14] Y. Bengio, "Learning Deep Architectures for AI," *Found Trends Mach. Learn.*, 2007, doi: 10.1561/2200000006
- [15] J. Deng, W. Dong et al., "ImageNet: A large-scale hierarchical image database," in *2009 IEEE Conference on Computer Vision and Pattern Recognition*, Jun. 2009, pp. 248–255. doi: 10.1109/CVPR.2009.5206848
- [16] P. Rasilo et al., "Simulink Model for PWM-Supplied Laminated Magnetic Cores Including Hysteresis, Eddy-Current, and Excess Losses," *IEEE Trans. Power Electron.*, vol. 34, no. 2, pp. 1683–1695, Feb. 2019